

FedMoE: Data-Level Personalization with Mixture of Experts for Model-Heterogeneous Personalized Federated Learning

Liping Yi
yiliping@nbjl.nankai.edu.cn
College of C.S., TMCC, SysNet,
DISSec, GTIISC, Nankai University
Tianjin, China

Han Yu
han.yu@ntu.edu.sg
School of Computer Science and
Engineering, Nanyang Technological
University (NTU)
Singapore

Chao Ren
chao.ren@ntu.edu.sg
School of Computer Science and
Engineering, Nanyang Technological
University (NTU)
Singapore

Heng Zhang
hengzhang@tju.edu.cn
College of Intelligence and
Computing, Tianjin University
Tianjin, China

Gang Wang
wgzwp@nbjl.nankai.edu.cn
College of C.S., TMCC, SysNet,
DISSec, GTIISC, Nankai University
Tianjin, China

Xiaoguang Liu
liuxg@nbjl.nankai.edu.cn
College of C.S., TMCC, SysNet,
DISSec, GTIISC, Nankai University
Tianjin, China

Xiaoxiao Li
xiaoxiao.li@ece.ubc.ca
Electrical and Computer Engineering
Department, University of British
Columbia (UBC)
Vancouver, Canada

ABSTRACT

Federated learning (FL) is widely employed for collaborative training on decentralized data but faces challenges like *data*, *system*, and *model heterogeneity*. This prompted the emergency of **model-heterogeneous personalized federated learning (MHPFL)**. However, concerns persist regarding data and model privacy, model performance, communication, and computational costs in current MHPFL methods. To tackle these concerns, we propose a novel model-heterogeneous personalized **Federated learning** algorithm (**FedMoE**) with the Mixture of Experts (**MoE**), renowned for enhancing large language models (LLMs). It assigns a shared homogeneous small feature extractor and a local gating network for each client’s local heterogeneous large model. (1) During local training, the local heterogeneous model’s feature extractor acts as a *local expert* for personalized feature (representation) extraction, while the shared homogeneous small feature extractor serves as a *global expert* for generalized feature extraction. The *local gating network* produces personalized weights for extracted representations from both experts on each data sample. The three models form a local heterogeneous *MoE*. The weighted mixed representation fuses global generalized and local personalized features and is processed by the local heterogeneous large model’s header with personalized prediction information for output. The *MoE* and prediction header are updated synchronously. (2) The trained local homogeneous small feature extractors are sent to the server for cross-client information fusion via aggregation. Briefly, FedMoE first **enhances local model personalization at a fine-grained data level while supporting model heterogeneity**. We theoretically prove FedMoE’s convergence over time. Extensive experiments demonstrate its superior

model performance, with up to 2.8% and 22.16% accuracy improvement over the state-of-the-art and the same-category best baselines, and lower computation and acceptable communication costs.

KEYWORDS

Personalized Federated Learning, Model Heterogeneity, Data Heterogeneity, System Heterogeneity, Mixture of Experts (MoE)

1 INTRODUCTION

Currently, efforts are focused on developing large-scale models and feeding them with massive data to improve model performances, like ChatGPT and AIGC. With growing concerns about privacy leaks, collecting decentralized data for training models is prohibited.

Federated learning [19, 29] is an emerging distributed machine learning paradigm where a server coordinates multiple clients to train a shared model without sharing data. In a typical FL algorithm - FedAvg [29], the server randomly selects a subnet of clients and sends them the global model. Each selected client initializes its local model with the global model and trains it on local data. The trained local models are then uploaded to the server for aggregation to generate a new global model by weighted averaging. Throughout FL, only model parameters are exchanged between the server and clients, avoiding data exposure as data are always stored in clients. However, this definition restricts clients and the server to maintain the same model structures, *i.e.*, **model homogeneity**.

Model homogeneity in typical FL faces challenges: (1) Decentralized data from clients are often non-independent and identically distributed (Non-IID), *i.e.*, **data or statistical heterogeneity**. A single shared global model trained on non-IID data may not adapt well to each client’s local data, sometimes performing worse than locally trained models. (2) In cross-device FL, clients are often edge mobile

devices with varying system configurations, such as bandwidth and computing power, *i.e.*, **system heterogeneity**. If all clients participate in FL, the model size must be compatible with the lowest-end device, causing performance bottlenecks and resource wastage on high-end devices. (3) In cross-silo FL, clients are institutions or enterprises concerned with protecting model intellectual property and maintaining different private model repositories, *i.e.*, **model heterogeneity**, they aim to further train existing private models through FL without revealing their structures. Therefore, enabling clients to train personalized and heterogeneous local models in FL *a.k.a.*, **Model-Heterogeneous Personalized Federated Learning (MHPFL)**, allows adaptation to local data distributions, system resources, and model structures, paving a new way for FL.

Existing MHPFL methods mainly fall into three branches: (1) Knowledge distillation-based MHPFL, which either relies on extra public data with similar distributions as local data or imposes computational and communication burdens on clients due to knowledge distillation. (2) Model mixup-based MHPFL splits client models into shared homogeneous and private heterogeneous parts, but sharing only the homogeneous part bottlenecks model performances and reveals model structures. (3) Mutual learning-based MHPFL alternately trains private heterogeneous large models and shared homogeneous small models for each client in a mutual learning manner, burdening client computation. The recent FedAPEN, based on mutual learning, enables each client to first train a personalized weight for its private heterogeneous large model output. Then each client fixes this weight and alternatively trains the homogeneous and heterogeneous models with weighted ensemble outputs. Although it trains a personalized weight for each client, *i.e.*, *client-level personalization*, it lacks a more fine-grained exploration of both generalized and personalized knowledge for each data sample, limiting model accuracy.

With the rapid development of large language models (LLMs), incorporating various data modalities like images and text increases training and inference costs. To address this for multimodal LLMs, besides increasing LLMs scales or fine-tuning, the **Mixture of Experts (MoE)** is proposed. An MoE (Figure 1) involves a gating network and multiple expert models. During training, a data sample passes through the gating network to produce weights for all experts. The top- p weighted experts process this sample, and their predictions weighted by corresponding weights form the final output. The loss between mixed outputs and labels updates p experts and the gating network synchronously. The key idea of MoE is to partition data into subtasks using the gating network, assigning specific experts to handle different subtasks based on their expertise. This allows MoE to address both general and specialized problems.

FedCP[47] highlights that each data sample contains both generalized and personalized information, with proportions varying across samples. Inspired by MoE’s dynamical expert weights for each data sample, we devise **FedMoE**, a novel **model-heterogeneous personalized Federated learning method** based on **MoE**, to enhance personalization at the **data level** and support **model heterogeneity**. Each client comprises a local gating network, a local heterogeneous large model’s feature extractor (*local expert*) for *personalized information extraction*, and a globally shared homogeneous small feature extractor (*global expert*) for *extracting generalized information*, forming a local MoE. 1) During local training,

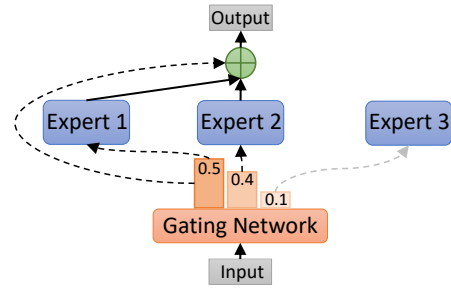


Figure 1: Workflow of MoE.

for each local data sample, the gating network adaptively produces personalized weights for the representations extracted by the two experts. The weighted mixed representation, incorporating both generalized and personalized feature information, is then processed by the local heterogeneous model’s prediction header involving personalized prediction information to output the prediction. The hard loss between predictions and labels *synchronously updates* MoE and the header. 2) After local training, the homogeneous small feature extractors are sent to the server for aggregating information from heterogeneous models.

Contributions. The main contributions are summarized as:

- We first employ MoE to enhance data-level personalization in model heterogeneous FL adaptive to non-IID data distributions, system resources, and model requirements.
- We theoretically prove that FedMoE can converge over time.
- Extensive experiments demonstrate that FedMoE obtains the state-of-the-art model accuracy while consuming lower computational and acceptable communication costs.

2 RELATED WORK

2.1 Model-Heterogeneous Personalized FL

Existing MHPFL has two families: (1) Clients train *heterogeneous local subnets* of the global model by model pruning, and the server aggregates them by parameter ordinate, such as FedRolex [3], HeteroFL [10], FjORD [13], HFL [26], Fed2 [44], FedResCuE [51]; (2) Clients hold *completely heterogeneous local models* and exchange knowledge with others by knowledge distillation, model mixture, and mutual learning. We focus on the latter, which exhibits higher model heterogeneity and is more prevalent in practice.

MHPFL with Knowledge Distillation. Cronus [4], FedGEMS [7], Fed-ET [8], FSFL [14], FCCL [15], DS-FL [16], FedMD [21], FedKT [22], FedDF [24], FedHeNN [28], FedAUX [35], CFD [36], FedKEMF [45] and KT-pFL [46], KRR-KD [32], FedKEM [30], pFedHR [41]) enable the server to aggregate same-dimension local logits or representations of an additional (labeled or unlabeled) public dataset with a similar distribution as local data to generate global logits or representations which are sent to clients for distillation loss calculation with local logits or representations. However, obtaining such a public dataset is impractical due to data privacy. Distillation on clients burdens computation, while communicating logits or representation of each public data sample between the server and clients burdens communication. To avoid using public data, FedZKT [48] and FedGen [50], FedGD [43] train a global generator to produce synthetic data for replacing public data, but generator training is time-consuming and

reduces FL efficiency. HFD [1, 2], FedGKT [12], FD [18], FedProto [39], and FedGH [43] do not rely on public or synthetic data. Instead, clients share seen classes and corresponding class-average logits or representations with the server, which are then distilled with global logits or representation of each class. However, these methods increase computational costs on clients and might be restricted in privacy-sensitive scenarios due to class uploading.

MHPFL with Model Mixture. A local model is split into a feature extractor and a classifier. FedMatch [6], FedRep [9], FedBABU [31] and FedAlt/FedSim [33] share homogeneous feature extractors while holding heterogeneous classifiers. FedClassAvg [17], LG-FedAvg [23] and CHFL [25] behave oppositely. They inherently only offer models with partial heterogeneity, potentially leading to performance bottlenecks and partial model structure exposure.

MHPFL with Mutual Learning. Each client in FML [38] and FedKD [42] has a local heterogeneous large model and a shared homogeneous small model, which are trained alternatively by mutual learning. The trained shared homogeneous small models are aggregated at the server to fuse information from different clients. However, alternative training increases computational burdens. Recent FedAPEN [34] improves FML by enabling each client to first learn a trainable weight λ for local heterogeneous model *outputs*, with $(1 - \lambda)$ is assigned to the shared homogeneous model outputs; then fixing this pair of weights and training two models with the ensemble loss between the weighted ensemble outputs and labels. Due to diverse data distributions among clients, the learnable weights are diverse, *i.e.*, achieving **client-level personalization**. Whereas, it fails to explore both generalized and personalized knowledge at the data level due to fixing weights during training.

Insight. FedMoE treats the shared homogeneous small feature extractor and the local heterogeneous large model's feature extractor as two experts of MoE, and employs a lightweight linear gating network to produce personalized weights for the *representations* of both experts for each data sample, enabling the extraction of both global generalized and local personalized knowledge at a more fine-grained **data-level personalization** that adapts to in-time data distribution, contrasting with FedAPEN's limited **client-level personalization**. Hence, FedMoE promotes model performance and supports federated continuous learning with distribution-drift streaming data, a feat beyond FedAPEN. Besides, FedMoE **synchronously** updates three models in MoE, saving training time compared to first training learnable weights and then **alternatively** training models in FedAPEN. Clients and the server in FedMoE only exchange homogeneous small feature extractors, reducing communication costs and preserving data and heterogeneous model privacy.

2.2 MoE and Federated Learning

PFL-MoE [11] first introduces *MoE* into *personalized FL* to mitigate data heterogeneity in *model-homogeneous* scenarios. In each round, each client receives the global model from the server as a *global expert* and fine-tunes it on *partial* local data as a *local expert*, the two experts and a gating network forms a MoE. During MoE training, each client utilizes a personalized gating network with only *one linear layer* to produce weights of the *outputs* of two experts. Then the weighted output is used for updating the local model and the gating network on *remaining* local data. Although alleviating

data heterogeneity through *data-level* personalization, it faces two constraints: (1) Training MoE on partial local data may compromise model performances. (2) The one-linear-layer gating network with few parameters might extract limited knowledge from local data.

In contrast to PFL-MoE, (1) FedMoE enhances data-level personalization in more challenging *model-heterogeneous* FL scenarios. (2) The gating network in FedMoE produces weights for two experts' *representations* carrying more information than outputs, facilitating the fusion of global generalized and local personalized feature. The weighted mixed representations are processed by the prediction header of local personalized heterogeneous models to enhance prediction personalization. (3) We devise a *more efficient gating network* to learn local data distributions. (4) We train the three models of MoE *synchronously* on *all* local data for boosting model performances and saving training time.

3 PRELIMINARIES

In a typical *model-homogeneous* FL algorithm - FedAvg [29], considering an FL system comprising a server and N clients. In each communication round, 1) the server randomly samples $K = C \cdot N$ clients \mathcal{S} (C , sampling ratio; K , number of sampled clients; \mathcal{S} , sampled client set, $|\mathcal{S}| = K$) and broadcasts the global model $\mathcal{F}(\omega)$ (\mathcal{F} , model structure; ω , model parameters) to the sampled K clients. 2) Client k initializes its local model $\mathcal{F}(\omega_k)$ with the received global model $\mathcal{F}(\omega)$ and train it on local data D_k ($D_k \sim P_k$, data from different clients obey diverse distributions, *i.e.*, non-IID) by $\omega_k \leftarrow \omega_k - \eta \omega \nabla \ell(\mathcal{F}(\mathbf{x}_i; \omega_k), y_i)$, $(\mathbf{x}_i, y_i) \in D_k$, then the updated local model $\mathcal{F}(\omega_k)$ is uploaded to the server. 3) The server aggregates the received local models to produce a global model by $\omega = \sum_{k \in \mathcal{S}} \frac{n_k}{n} \omega_k$ ($n_k = |D_k|$, the sample size of client- k 's local data D_k ; n is sample size across all clients). Repeating the above steps until the global model converges. Typical FL aims to minimize the average loss of the global model on local data across all clients, *i.e.*,

$$\min_{\omega} \sum_{k=0}^{N-1} \frac{n_k}{n} \ell(\mathcal{F}(D_k; \omega)). \quad (1)$$

This definition requires all clients and the server to possess models with identical structures $\mathcal{F}(\cdot)$, *i.e.*, **model-homogeneous**.

FedMoE aims to realize **model-heterogeneous** personalized for in supervised learning tasks. We define client k 's local heterogeneous model as $\mathcal{F}_k(\omega_k)$ ($\mathcal{F}_k(\cdot)$, heterogeneous model structure; ω_k , personalized model parameters). The objective is to minimize the sum of the loss of local heterogeneous models on local data, *i.e.*,

$$\min_{\omega_0, \dots, \omega_{N-1}} \sum_{k=0}^{N-1} \ell(\mathcal{F}_k(D_k; \omega_k)). \quad (2)$$

4 THE PROPOSED FEDMOE ALGORITHM

Motivation. In FL, the global model has ample generalized knowledge, while local models have personalized knowledge. Participating clients, with limited local data, hope to enhance the generalization of local models to improve model performances. For client k , its local heterogeneous model $\mathcal{F}_k(\omega_k)$ comprises a feature extractor $\mathcal{F}_k^{ex}(\omega_k^{ex})$ and a prediction header $\mathcal{F}_k^{hd}(\omega_k^{hd})$, $\mathcal{F}_k(\omega_k) =$

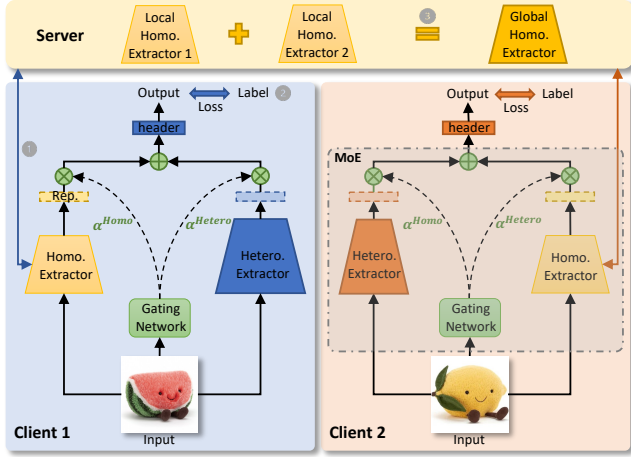


Figure 2: Workflow of FedMoE.

$\mathcal{F}_k^{ex}(\omega_k^{ex}) \circ \mathcal{F}_k^{hd}(\omega_k^{hd})$. The feature extractor captures *low-level personalized feature information*, while the prediction header incorporates *high-level personalized prediction information*. Hence, (1) **we enhance the generalization of the local heterogeneous feature extractor** to extract more generalized features through FL, while retaining the prediction header of the local heterogeneous model to enhance personalized prediction capabilities. Furthermore, Zhang et al. [47] highlights that various local data samples of a client contain differing proportions of global generalized information and local personalized information. This motivates us to (2) **dynamically balance the generalization and personalization of local heterogeneous models, adapting to non-IID data across different clients at the data level**.

Overview. To implement the above insights, FedMoE incorporates a shared small homogeneous feature extractor $\mathcal{G}(\theta)$ far smaller than the local heterogeneous feature extractor $\mathcal{F}_k^{ex}(\omega_k^{ex})$. As displayed in Figure. 2, in the t -th communication round, the workflow of FedMoE involves the following steps:

- (1) The server randomly samples K clients \mathcal{S}^t and sends the global homogeneous small feature extractor $\mathcal{G}(\theta^{t-1})$ aggregated in the $(t-1)$ -th round to them.
- (2) Client $k \in \mathcal{S}^t$ regards the received global homogeneous small feature extractor $\mathcal{G}(\theta^{t-1})$ as the *global expert* for extracting *generalized feature across all classes*, and treats the local heterogeneous large feature extractor $\mathcal{F}_k^{ex}(\omega_k^{ex,t-1})$ as the *local expert* for extracting *personalized feature of local seen classes*. A (homogeneous or heterogeneous) lightweight personalized *local gating network* $\mathcal{H}(\varphi_k^{t-1})$ is introduced to balance generalization and personalization by dynamically producing weights for each sample's representations from two experts. The three models form a *MoE architecture*. The weighted mixed representation from MoE is then processed by the local heterogeneous large model's prediction header $\mathcal{F}_k^{hd}(\omega_k^{hd,t-1})$ to extract *personalized prediction information*.

The three models in MoE and the header are trained synchronously in an *end-to-end* manner. The updated homogeneous $\mathcal{G}(\theta_k^t)$ is uploaded to the server, while $\mathcal{F}_k(\omega_k^t)$, $\mathcal{H}(\varphi_k^t)$ are retained in clients.

- (3) The server aggregates the received local homogeneous feature extractors $\mathcal{G}(\theta_k^t)$ ($k \in \mathcal{S}^t$) by weighted averaging to produce a new global homogeneous feature extractor $\mathcal{G}(\theta^t)$.

The above process iterates until all local heterogeneous *complete models* (MoE and prediction header) converge. At the end of FL, local heterogeneous complete models are used for **inference**. The detailed algorithm is illustrated in Algorithm 1 (Appendix A).

4.1 MoE Training

In MoE, each local data sample $(x_i, y_i) \in D_k$ is fed into the global expert $\mathcal{G}(\theta^{t-1})$ with global generalized feature knowledge to produce the *generalized representation*, and simultaneously into the local expert $\mathcal{F}_k^{ex}(\omega_k^{ex,t-1})$ to generate the *personalized representation*,

$$\mathcal{R}_{k,i}^{\mathcal{G},t} = \mathcal{G}(x_i; \theta^{t-1}), \mathcal{R}_{k,i}^{\mathcal{F},t} = \mathcal{F}_k^{ex}(x_i; \omega_k^{ex,t-1}). \quad (3)$$

Each local data sample $(x_i, y_i) \in D_k$ is also fed into the local gating network $\mathcal{H}(\varphi_k^{t-1})$ to produce weights for two experts,

$$[\alpha_{k,i}^{\mathcal{G},t}, \alpha_{k,i}^{\mathcal{F},t}] = \mathcal{H}(x_i; \varphi_k^{t-1}), \alpha_{k,i}^{\mathcal{G},t} + \alpha_{k,i}^{\mathcal{F},t} = 1. \quad (4)$$

Notice that different clients can hold heterogeneous gating networks $\mathcal{H}_k(\varphi_k)$ with the same input dimension d as local data sample x and the same output dimension $h = 2$. We use homogeneous gating networks $\mathcal{H}(\varphi_k)$ for all clients in this paper.

Then we mix the representations of two experts with the weights produced by the gating network,

$$\mathcal{R}_{k,i}^t = \alpha_{k,i}^{\mathcal{G},t} \cdot \mathcal{R}_{k,i}^{\mathcal{G},t} + \alpha_{k,i}^{\mathcal{F},t} \cdot \mathcal{R}_{k,i}^{\mathcal{F},t}. \quad (5)$$

To enable the above representation mixture, we require that the last layer dimensions of the homogeneous small feature extractor and the heterogeneous large feature extractor are identical.

The mixed representation $\mathcal{R}_{k,i}^t$ is then processed by the local personalized prediction header $\mathcal{F}_k^{hd}(\omega_k^{hd,t-1})$ (both homogeneous and heterogeneous header are allowed, we use homogeneous headers in this work) to produce prediction,

$$\hat{y}_i = \mathcal{F}_k^{hd}(\mathcal{R}_{k,i}^t; \omega_k^{hd,t-1}). \quad (6)$$

We calculate the hard loss (e.g. Cross-Entropy loss [49]) between the prediction and the label,

$$\ell_i = CE(\hat{y}_i, y_i). \quad (7)$$

Then we update all models synchronously by gradient descent (e.g., SGD optimizer) in an end-to-end manner,

$$\begin{aligned} \theta_k^t &\leftarrow \theta_k^{t-1} - \eta_\theta \nabla \ell_i, \\ \omega_k^t &\leftarrow \omega_k^{t-1} - \eta_\omega \nabla \ell_i, \\ \varphi_k^t &\leftarrow \varphi_k^{t-1} - \eta_\varphi \nabla \ell_i. \end{aligned} \quad (8)$$

$\eta_\theta, \eta_\omega, \eta_\varphi$ are the learning rates of the homogeneous small feature extractor, the heterogeneous large model, and the gating network. To enable stable convergence, we set $\eta_\theta = \eta_\omega$.

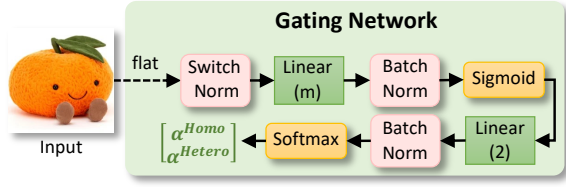


Figure 3: Gating network structure.

4.2 Homogeneous Extractor Aggregation

After local training, client $k \in \mathcal{S}^t$ uploads its local homogeneous small feature extractor θ_k^t to the server. The server then aggregates them by weighted averaging to produce a new global homogeneous small feature extractor,

$$\theta^t = \sum_{k \in \mathcal{S}^t} \frac{n_k}{n} \theta_k^t. \quad (9)$$

Problem Re-formulation. The local personalized gating networks of different clients dynamically produce weights for the representations of two experts on each sample of local non-IID data, balancing the generalization and personalization adaptive to local data distributions. Thus, FedMoE enhances personalization of model-heterogeneous personalized FL at the fine-grained **data level**. Therefore, the objective defined in Eq. (2) can be specified as

$$\min_{\omega_0, \dots, \omega_{N-1}} \sum_{k=0}^{N-1} \ell(\mathcal{F}_k^{hd}(\mathcal{G}(D_k; \theta), \mathcal{F}_k^{ex}(D_k; \omega_k^{ex})) \cdot \mathcal{H}(D_k; \varphi_k); \omega_k^{hd}). \quad (10)$$

$\mathcal{H}(D_k; \varphi_k)$ denotes the weights $[\alpha^{\mathcal{G}}, \alpha^{\mathcal{F}_k}]$ of two experts. \cdot is dot product, *i.e.*, summing after element-wise multiplication.

4.3 Gating Network

The local gating network $\mathcal{H}(\varphi_k)$ takes each data sample $x_i \in D_k$ as input outputs two weights $[\alpha_{k,i}^{\mathcal{G}}, \alpha_{k,i}^{\mathcal{F}_k}]$ (summing to 1) for the representations of two experts, as defined in Eq. (4). A *linear network* is the simplest model fulfilling these functions. Therefore, we customize a dedicated lightweight linear gating network for FedMoE, depicted in Figure 3.

Linear Layer. FedMoE trains models in *batches*. When processing a batch of color image samples, the input dimension is $[\text{length}, \text{width}, \text{channel} = 3, \text{batchsize}]$. Before feeding it into the gating network, we flatten it to a vector with $[(\text{length} \cdot \text{width} \cdot 3, \text{batchsize})]$ pixels. Given the large input vector, a gating network with only one linear layer containing 2 neurons might not efficiently capture local data knowledge and could be prone to overfitting due to limited parameter capacity. Hence, we employ 2 linear layers for the gating network: the first layer with m neurons ($\text{length} \cdot \text{width} \cdot 3 \cdot m$ parameters), and the second layer with 2 neurons ($m \cdot 2$ parameters).

Normalization. Normalization techniques are commonly employed in deep neuron networks for regularization to improve model generalization and accelerate training. Common approaches include *batch*, *instance*, and *layer normalization*. Recently, *switch normalization*, proposed by Luo et al. [27], integrates the advantages of these typical methods and efficiently handles batch data with diverse characteristics [5]. After flattening the input, we apply a switch normalization layer before feeding it into the first linear layer. To leverage the benefits of widely used *batch normalization*, we include batch normalization layers after two linear layers.

Activation Function. Activation functions increase non-linearity to improve deep network expression, mitigating gradient vanishing or explosion. Commonly used activations include: *Sigmoid*, *ReLU*, *Softmax*, *etc*, each with its own range of values. Since the gating network's output weights range between 0 and 1, we add a *Sigmoid* activation layer after the first linear layer to confine its output within $(0, 1)$. We add a *Softmax* activation layer after the second linear layer to ensure that the produced two weights sum to 1.

4.4 Discussion

Model Performance. FedMoE effectively balances generalization and personalization by fine-grained data-level personalization adapting to local non-IID data distribution, thereby boosting model performances. Moreover, it is suitable for federated continuous learning scenarios with distribution-drift streaming data.

Privacy. Clients share the homogeneous small feature extractors for knowledge exchange. Local heterogeneous large models and local data remain stored on clients, preserving their privacy.

Communication. Only homogeneous small feature extractors are transmitted between the server and clients, consuming lower communication costs than transmitting complete models in FedAvg.

Computation. Apart from training local heterogeneous large models, clients also train a small homogeneous feature extractor and a lightweight linear gating network. However, due to the smaller sizes of them than the heterogeneous large feature extractor, the computational overheads are acceptable. Moreover, simultaneous training of MoE and the prediction header reduces training time.

5 ANALYSIS

We first clarify additional notations used for analysis in Table 1.

Table 1: Description of Additional Notations.

Notation	Description
$t \in \{0, \dots, T-1\}$	communication round
$e \in \{0, 1, \dots, E\}$	local iteration
$tE + 0$	before the $(t+1)$ -th round's local training, client k receives the global homogeneous small feature extractor $\mathcal{G}(\theta^t)$ aggregated in the t -th round
$tE + e$	the e -th local iteration in the $(t+1)$ -th round
$tE + E$	the last local iteration, after that, client k uploads the local homogeneous small feature extractor to the server
W_k	client k 's local complete model involving the MoE $(\{\mathcal{G}(\theta), \mathcal{F}_k^{ex}(\omega_k^{ex}), \mathcal{H}(\varphi_k)\})$ and the prediction header $\mathcal{F}_k^{hd}(\omega_k^{hd})$
η	the learning rate of the client k 's local complete model W_k , involving $\{\eta_\theta, \eta_\omega, \eta_\varphi\}$

ASSUMPTION 1. Lipschitz Smoothness. Gradients of client k 's local complete heterogeneous model W_k are L_1 -Lipschitz smooth [39],

$$\|\nabla \mathcal{L}_k^{t_1}(W_k^{t_1}; \mathbf{x}, \mathbf{y}) - \nabla \mathcal{L}_k^{t_2}(W_k^{t_2}; \mathbf{x}, \mathbf{y})\| \leq L_1 \|W_k^{t_1} - W_k^{t_2}\|, \quad (11)$$

$$\forall t_1, t_2 > 0, k \in \{0, 1, \dots, N-1\}, (\mathbf{x}, \mathbf{y}) \in D_k.$$

The above formulation can be derived further as:

$$\mathcal{L}_k^{t_1} - \mathcal{L}_k^{t_2} \leq \langle \nabla \mathcal{L}_k^{t_2}, (W_k^{t_1} - W_k^{t_2}) \rangle + \frac{L_1}{2} \|W_k^{t_1} - W_k^{t_2}\|_2^2. \quad (12)$$

ASSUMPTION 2. Unbiased Gradient and Bounded Variance. Client k 's random gradient $g_{W,k}^t = \nabla \mathcal{L}_k^t(W_k^t; \mathcal{B}_k^t)$ (\mathcal{B} is a batch of local data) is unbiased,

$$\mathbb{E}_{\mathcal{B}_k^t \in D_k} [g_{W,k}^t] = \nabla \mathcal{L}_k^t(W_k^t), \quad (13)$$

and the variance of random gradient $g_{W,k}^t$ is bounded by:

$$\mathbb{E}_{\mathcal{B}_k^t \in D_k} [\|\nabla \mathcal{L}_k^t(W_k^t; \mathcal{B}_k^t) - \nabla \mathcal{L}_k^t(W_k^t)\|_2^2] \leq \sigma^2. \quad (14)$$

ASSUMPTION 3. Bounded parameter variation. The parameter variations of the homogeneous small feature extractor θ_k^t and θ^t before and after aggregation is bounded as

$$\|\theta^t - \theta_k^t\|_2^2 \leq \delta^2. \quad (15)$$

Based on the above assumptions, we can derive the following Lemma and Theorem, and their proofs are given in Appendix B.

LEMMA 1. Local training. Given Assumptions 1 and 2, the loss of an arbitrary client's local model W in the $(t+1)$ -th round's local training is bounded by

$$\mathbb{E}[\mathcal{L}_{(t+1)E}] \leq \mathcal{L}_{tE+0} + \left(\frac{L_1\eta^2}{2} - \eta\right) \sum_{e=0}^E \|\nabla \mathcal{L}_{tE+e}\|_2^2 + \frac{L_1E\eta^2\sigma^2}{2}. \quad (16)$$

LEMMA 2. Model Aggregation. Given Assumption 2 and 3, after the $(t+1)$ -th round's local training, the loss of any client before and after aggregating local homogeneous small feature extractors at the server is bounded by

$$\mathbb{E}[\mathcal{L}_{(t+1)E+0}] \leq \mathbb{E}[\mathcal{L}_{tE+1}] + \eta\delta^2. \quad (17)$$

THEOREM 1. One complete round of FL. Based on Lemma 1 and Lemma 2, for any client, after local training, model aggregation, and receiving the new global homogeneous feature extractor, we can obtain

$$\mathbb{E}[\mathcal{L}_{(t+1)E+0}] \leq \mathcal{L}_{tE+0} + \left(\frac{L_1\eta^2}{2} - \eta\right) \sum_{e=0}^E \|\nabla \mathcal{L}_{tE+e}\|_2^2 + \frac{L_1E\eta^2\sigma^2}{2} + \eta\delta^2. \quad (18)$$

THEOREM 2. Non-convex convergence rate of FedMoE. Based on Theorem 1, for any client and an arbitrary constant $\epsilon > 0$, satisfying

$$\frac{1}{T} \sum_{t=0}^{T-1} \sum_{e=0}^{E-1} \|\nabla \mathcal{L}_{tE+e}\|_2^2 \leq \frac{\frac{1}{T} \sum_{t=0}^{T-1} [\mathcal{L}_{tE+0} - \mathbb{E}[\mathcal{L}_{(t+1)E+0}]] + \frac{L_1E\eta^2\sigma^2}{2} + \eta\delta^2}{\eta - \frac{L_1\eta^2}{2}} < \epsilon, \\ \text{s.t. } \eta < \frac{2(\epsilon - \delta^2)}{L_1(\epsilon + E\sigma^2)}. \quad (19)$$

Therefore, any client's local model can converge with a non-convex rate $\epsilon \sim \mathcal{O}(\frac{1}{T})$.

6 EXPERIMENTAL EVALUATION

We implement FedMoE and baselines using Pytorch and conduct experiments on 4 NVIDIA GeForce RTX 3090 GPUs.

6.1 Experiment Setup

Datasets. We evaluate FedMoE and baselines on CIFAR-10 and CIFAR-100¹ [20] image classification benchmark datasets. CIFAR-10 comprises 6000 32×32 color images across 10 classes, with 5000 images in the training set and 1000 images in the testing set. CIFAR-100 contains 100 classes of color images, each with 500 training images and 100 testing images. To construct non-IID datasets, we employ two data partitioning strategies: (1) **Pathological.** Following Shamsian et al. [37], we allocate 2 classes to each client on CIFAR-10 and use Dirichlet distribution to generate varying counts of the same class for different clients, denoted as (Non-IID: 2/10); and we assign 10 classes to each client on CIFAR-100, marked as (Non-IID: 10/100). (2) **Practical.** Referred to Qin et al. [34], we allocate all classes to each client and utilize Dirichlet distribution(γ) to control the proportions of each class across clients. After non-IID

division, each client's local data is divided into training and testing sets in an 8 : 2 ratio, ensuring both sets follow the same distribution.

Models. We assess FedMoE and baselines in model-homogeneous and model-heterogeneous FL scenarios. For model-homogeneous settings, all clients hold the same CNN-1 shown in Table 4 (Appendix C). In model-heterogeneous settings, 5 heterogeneous CNN models are evenly allocated to different clients, with assignment IDs determined by client ID modulo 5.

Baselines. We compare FedMoE against state-of-the-art MHPFL algorithms from the most relevant three categories of public data-independent MHPFL algorithms outlined in Section 2.

- **Standalone.** Clients solely utilize their local data to train local models without FL process.
- **MHPFL with Knowledge Distillation:** FD [18], FedProto [39].
- **MHPFL with Model Mixture:** LG-FedAvg [23].
- **MHPFL with Mutual Learning:** FML [38], FedKD [42], and the latest FedAPEN [34]. FedMoE belongs to this category.

Metrics. We measure the model performances, communication costs, and computational overheads of all algorithms.

- **Model Performances.** We evaluate each client's local model's **individual testing accuracy** on the local testing set and calculate their **mean testing accuracy**.
- **Communication Costs.** We monitor the communication rounds required to reach **target mean accuracy** and quantify communication costs by multiplying rounds with the mean parameter capacity transmitted in one round.
- **Computational Overheads.** We calculate computational overheads by multiplying the communication rounds required to achieve **target mean accuracy** with the local mean computational FLOPs in one round.

Training Strategy. We conduct a grid search to identify the optimal FL settings and specific hyperparameters for all algorithms. In FL settings, we evaluate all algorithms with total communication rounds $T = \{100, 500\}$, local epochs $\{1, 10\}$, batch size $\{64, 128, 256, 512\}$ and SGD optimizer with learning rate $\{0.001, 0.001, 0.1, 1\}$. For FedMoE, the homogeneous small feature extractor and the heterogeneous large model have the same learning rate, *i.e.*, $\eta_\theta = \eta_\omega$. We report the highest accuracy achieved for all algorithms.

6.2 Comparisons Results

To test algorithms in different FL scenarios with varying numbers of clients N and client participation rates C , we design three settings: $\{(N = 10, C = 100\%), (N = 50, C = 20\%), (N = 100, C = 10\%)\}$.

6.2.1 Model Homogeneity. This is a special case of model heterogeneity. Table 2 shows that FedMoE *consistently achieves the highest accuracy*, surpassing 1.74% compared with each setting's state-of-the-art baseline (LG-FedAvg, Standalone, Standalone, FedProto, Standalone, Standalone), and improving 5.47% accuracy compared with the same-category best baseline FedAPEN, FedAPEN, FedAPEN, FedAPEN, FedKD, FedKD, indicating that FedMoE efficiently boosts model accuracy through adaptive data-level personalization.

6.2.2 Model Heterogeneity. In this scenario, FedMoE and other mutual learning-based MHPFL baselines utilize the smallest CNN-5 (Table 4, Appendix C) as homogeneous feature extractors or models.

¹<https://www.cs.toronto.edu/%7Ekriz/cifar.html>

Table 2: Mean testing accuracy in model-homogeneous FL scenarios. “-” denotes failure to converge.

FL Setting	N=10, C=100%		N=50, C=20%		N=100, C=10%	
	CIFAR-10	CIFAR-100	CIFAR-10	CIFAR-100	CIFAR-10	CIFAR-100
Standalone	96.35	74.32	95.25	62.38	92.58	54.93
LG-FedAvg	96.47	73.43	94.20	61.77	90.25	46.64
FD	96.30	-	-	-	-	-
FedProto	95.83	72.79	95.10	62.55	91.19	54.01
FML	94.83	70.02	93.18	57.56	87.93	46.20
FedKD	94.77	70.04	92.93	57.56	90.23	50.99
FedAPEN	95.38	71.48	93.31	57.62	87.97	46.85
FedMoE	96.80	76.06	95.80	63.06	93.55	56.46
FedMoE-Best B.	0.33	1.74	0.55	0.51	0.97	1.53
FedMoE-Best S.C.B.	1.42	4.58	2.49	5.44	3.32	5.47

Table 3: Mean accuracy in model-heterogeneous FL scenarios.

FL Setting	N=10, C=100%		N=50, C=20%		N=100, C=10%	
	CIFAR-10	CIFAR-100	CIFAR-10	CIFAR-100	CIFAR-10	CIFAR-100
Standalone	96.53	72.53	95.14	62.71	91.97	53.04
LG-FedAvg	96.30	72.20	94.83	60.95	91.27	45.83
FD	96.21	-	-	-	-	-
FedProto	96.51	72.59	95.48	62.69	92.49	53.67
FML	30.48	16.84	-	21.96	-	15.21
FedKD	80.20	53.23	77.37	44.27	73.21	37.21
FedAPEN	-	-	-	-	-	-
FedMoE	96.58	75.39	95.84	63.30	93.07	54.78
FedMoE-Best B.	0.05	2.80	0.36	0.59	0.58	1.11
FedMoE-Best S.C.B.	16.38	22.16	18.47	19.03	19.86	17.57

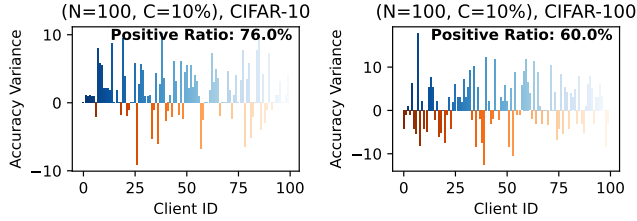


Figure 4: Accuracy distribution for individual clients.

Mean Accuracy. Table 3 manifests that FedMoE consistently outperforms baselines, improving up to 2.8% accuracy than each setting’s state-of-the-art baseline Standalone, FedProto, FedProto, Standalone, FedProto, FedProto, and increasing up to 22.16% accuracy than the same-category best baseline FedKD, again demonstrating the superiority of FedMoE in model performances. Figure 11 (Appendix C) depicts that FedMoE exhibits faster convergence speeds and higher model accuracy across most FL settings, particularly noticeable on CIFAR-100.

Individual Accuracy. Figure 4 depicts the individual accuracy discrepancy of each client in FedMoE and the state-of-the-art baseline - FedProto under ($N = 100, C = 10\%$). Most clients (CIFAR-10: 76%, CIFAR-100: 60%) in FedMoE perform higher accuracy than FedProto, again demonstrating that FedMoE with data-level personalization dynamically adapts to local data distribution and learns more generalized and personalized knowledge from local data, hence promoting personalized heterogeneous model accuracy.

Personalization Analysis. To explore the personalization level of FedMoE and FedProto, we extract the representation of each local data sample from each client produced by FedMoE’s local heterogeneous MoE and FedProto’s local heterogeneous feature extractor on CIFAR-10 (non-IID: 2/10) under ($N = 100, C = 10\%$). We employ T-SNE [40] technique to compress extracted representations to 2-dimension vectors and visualize them in Figure 5. Limited by plotting spaces, more clients $N = \{50, 100\}$ and CIFAR-100 with 100 classes can not be clearly depicted. Figure 5 displays that

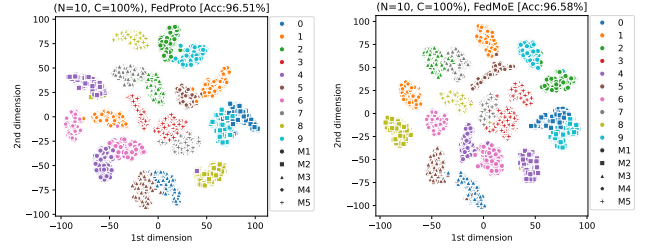


Figure 5: T-SNE representation visualization results for FedProto and FedMoE on CIFAR-10 (Non-IID: 2/10).

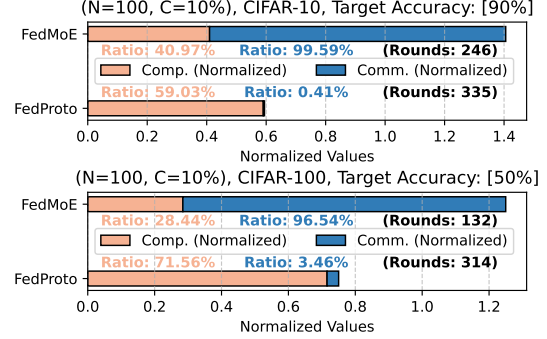


Figure 6: Computation, communication, and rounds required for reaching target mean accuracy.

representations from one client’s 2 seen classes keep close, while representations from different clients keep away, indicating that two algorithms indeed yield personalized local heterogeneous models. Regarding representations of one client’s 2 classes, they present “intra-class compactness, inter-class separation”, signifying a strong classification capability. Notably, representations of one client’s 2 classes in FedMoE exhibit clearer decision boundaries, i.e., representations within the same cluster are more compact, suggesting better classification performance and higher personalization level.

Communication and Computation. Figure 6 shows the required rounds, consumed communication, and computation in FedMoE and FedProto for reaching 90% and 50% target accuracy under the most complex ($N = 100, C = 10\%$). To facilitate comparisons, we normalize communication and computation, considering their different dimensions (number of parameters, FLOPs). **Computation.** FedMoE incurs lower computational costs than FedProto. Because FedProto requires extracting representations for all local data samples after training local heterogeneous models, while FedMoE trains an MoE and the prediction header synchronously for time-saving. One round of computation in FedMoE is less than FedProto, and since FedMoE requires fewer rounds to reach target accuracy, it incurs lower total computational costs. **Communication.** FedMoE incurs higher communication costs than FedProto. Because, in one round, clients in FedProto transmit seen-class representations with the server, while clients in FedMoE transmit homogeneous small feature extractors. So the former consumes lower communication costs than the latter per round. Despite requiring fewer rounds to reach target accuracy, FedMoE still consumes higher total communication costs. However, compared with transmitting complete local models in FedAvg, FedMoE still has lower communication overheads. Therefore, FedMoE exhibits more efficient computation and acceptable communication while delivering superior model accuracy.

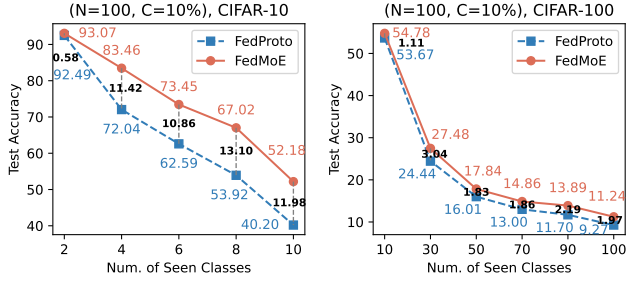


Figure 7: Robustness to *pathological non-IIDness*.

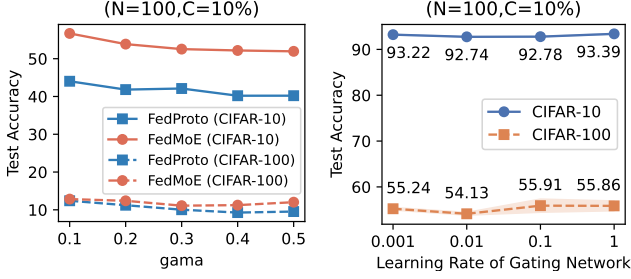


Figure 8: Left: robustness to *practical non-IIDness*. Right: sensitivity to the gating network’s learning rate.

6.3 Case Studies

6.3.1 Robustness to Pathological Non-IIDness. In model heterogeneous FL with $(N = 100, C = 10\%)$, the number of seen classes assigned to one client varies as $\{2, 4, 6, 8, 10\}$ on CIFAR-10 and $\{10, 30, 50, 70, 90, 100\}$ on CIFAR-100. Figure 7 shows that model accuracy drops as non-IIDness reduces (number of seen classes rises), as clients with more classes exhibit degraded classification ability for each class, *i.e.*, model generalization improves but personalization compromises. Besides, FedMoE consistently performs higher accuracy than FedProto across non-IIDnesses, indicating FedMoE is more robust to pathological non-IIDness. Moreover, FedMoE exhibits higher accuracy improvements compared to FedProto under IID than non-IID, *e.g.*, +13.10% on CIFAR-10 (Non-IID: 8/10) and +3.04% on CIFAR-100 (Non-IID: 30/100). This suggests that FedProto is more effective under non-IID than IID, consistent with the behavior in most personalized FL algorithms [34], while FedMoE adapts to both IID and non-IID by using a personalized gating network to dynamically balance global generalization and local personalization.

6.3.2 Robustness to Practical Non-IIDness. In model heterogeneous FL with $(N = 100, C = 10\%)$, γ in Dirichlet distribution varies as $\{0.1, 0.2, 0.3, 0.4, 0.5\}$. Figure 8 (left) shows that FedMoE consistently maintains higher accuracy than FedProto, indicating that FedMoE is more robust to practical Non-IIDness. Similar to the phenomena in Figure 7, model accuracy drops as non-IIDness reduces (γ rises), and FedMoE improves more accuracy under IID than non-IID.

6.3.3 Sensitivity to Hyperparameter. Only one extra hyperparameter - the learning rate η_ϕ of the gating network is introduced in FedMoE. In model heterogeneous FL with $(N = 100, C = 10\%)$, we evaluate FedMoE with $\eta_\phi = \{0.001, 0.01, 0.1, 1\}$ on CIFAR-10 (Non-IID: 2/10) and CIFAR-100 (Non-IID: 10/100). We randomly choose three random seeds to execute 3 trails for each test, and Figure 8 (right) depicts the accuracy mean (dots) and variation (shadow).

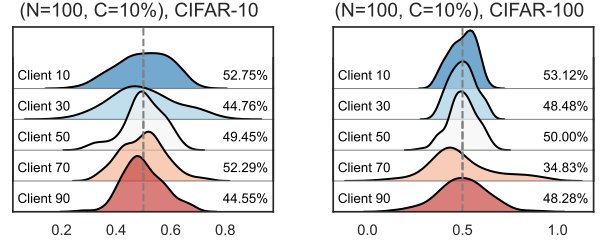


Figure 9: Produced weight distributions vary as *clients*.

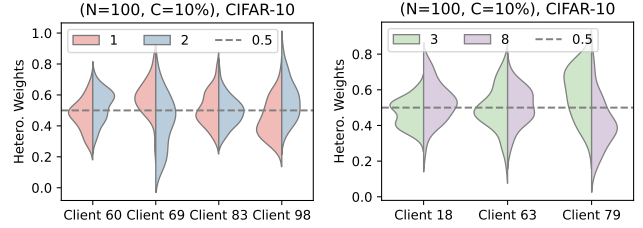


Figure 10: Produced weight distributions vary as *classes*.

FedMoE performs stable accuracy across varying gating network’s learning rates, indicating that FedMoE is not sensitive to η_ϕ .

6.3.4 Weights Analysis. We analyze FedMoE’s gating network’s output weights in model heterogeneous FL with $(N = 100, C = 10\%)$ on CIFAR-10 (Non-IID: 2/10) and CIFAR-100 (Non-IID: 10/100).

Client Perspective. We randomly select 5 clients and visualize the probability distribution of the weights produced by the final local gating network for the local personalized heterogeneous large feature extractor on all local testing data. Figure 9 shows that *different clients with non-IID data perform diverse weight distributions*, indicating that the weights produced by the local personalized gating network for different clients are indeed personalized and adaptive to local data distributions. Besides, *most weights are concentrated around 50%*, with some exceeding 50%, suggesting that the generalized features extracted by the homogeneous small feature extractor and the personalized features extracted by the heterogeneous large feature extractor contribute comparably to improve model performances, and the personalized output weights dynamically balance the generalization and the personalization.

Class Perspective. Upon identifying client sets with the same seen classes, we find 4 clients sharing classes [1, 2] and 3 clients sharing classes [3, 8] on CIFAR-10, but no clients have overlapping seen classes on CIFAR-100 since 100 classes are assigned to 100 clients. Figure 10 presents that *one class across different clients performs various weight distributions* and *different classes within one client also exhibit diverse weight distributions*, highlighting that FedMoE indeed implement data-level personalization.

7 CONCLUSIONS AND FUTURE WORK

This work proposed a novel model-heterogeneous personalized federated learning algorithm (FedMoE) with data-level personalization via a mixture of experts. Each client’s local complete model consists of a heterogeneous MoE (a share homogeneous small feature extractor (global expert), a local heterogeneous large model’s feature extractor (local expert), a local personalized gating network) and a local personalized prediction header. During training, the local

personalized gating network produces the weights for the representations of two experts on each local data sample, then the weighted mixed representation absorbing generalized feature and personalized feature is processed by the local personalized prediction header with abundant personalized prediction information to produce the prediction. The hard loss between the prediction and the label is used to update the MoE and the header synchronously in an end-to-end manner. After local training, the local homogeneous small feature extractors are uploaded to the server for aggregation to generate a new global feature extractor. To sum up, FedMoE exchanges knowledge from local heterogeneous models across different clients by sharing homogeneous small feature extractors, and it achieves data-level personalization adaptive to local non-IID data distribution by MoE to balance generalized and personalization. Theoretical analysis proves its $\mathcal{O}(1/T)$ non-convex convergence rate. Extensive experiments demonstrate that FedMoE obtains the state-of-the-art model accuracy while lower computation overheads and acceptable communication costs.

In future, we will further explore how FedMoE performs in federated continuous learning (FCL) scenarios with distribution-drift streaming data and improve it to adapt to practical FCL applications.

REFERENCES

- [1] Jin-Hyun Ahn et al. 2019. Wireless Federated Distillation for Distributed Edge Learning with Heterogeneous Data. In *Proc. PIMRC*. IEEE, Istanbul, Turkey, 1–6.
- [2] Jin-Hyun Ahn et al. 2020. Cooperative Learning VIA Federated Distillation OVER Fading Channels. In *Proc. ICASSP*. IEEE, Barcelona, Spain, 8856–8860.
- [3] Samiul Alam et al. 2022. FedRolex: Model-Heterogeneous Federated Learning with Rolling Sub-Model Extraction. In *Proc. NeurIPS*, virtual.
- [4] Hongyan Chang et al. 2021. Cronus: Robust and Heterogeneous Collaborative Learning with Black-Box Knowledge Transfer. In *Proc. NeurIPS Workshop*, virtual.
- [5] Daoyuan Chen et al. 2023. Efficient Personalized Federated Learning via Sparse Model-Adaptation. In *Proc. ICML*, Vol. 202. PMLR, Honolulu, Hawaii, USA, 5234–5256.
- [6] Jianguo Chen et al. 2021. FedMatch: Federated Learning Over Heterogeneous Question Answering Data. In *Proc. CIKM*. ACM, virtual, 181–190.
- [7] Sijie Cheng et al. 2021. FedGEMS: Federated Learning of Larger Server Models via Selective Knowledge Fusion. *CoRR* abs/2110.11027 (2021).
- [8] Yae Jee Cho et al. 2022. Heterogeneous Ensemble Knowledge Transfer for Training Large Models in Federated Learning. In *Proc. IJCAI*. ijcai.org, virtual, 2881–2887.
- [9] Liam Collins et al. 2021. Exploiting Shared Representations for Personalized Federated Learning. In *Proc. ICML*, Vol. 139. PMLR, virtual, 2089–2099.
- [10] Enmao Diao. 2021. HeteroFL: Computation and Communication Efficient Federated Learning for Heterogeneous Clients. In *Proc. ICLR*. OpenReview.net, Virtual Event, Austria, 1.
- [11] Binbin Guo et al. 2021. PFL-MoE: Personalized Federated Learning Based on Mixture of Experts. In *Proc. APWeb-WAIM*, Vol. 12858. Springer, Guangzhou, China, 480–486.
- [12] Chaoyang He et al. 2020. Group Knowledge Transfer: Federated Learning of Large CNNs at the Edge. In *Proc. NeurIPS*, virtual.
- [13] S. Horváth. 2021. FJORD: Fair and Accurate Federated Learning under heterogeneous targets with Ordered Dropout. In *Proc. NIPS*. OpenReview.net, Virtual, 12876–12889.
- [14] Wenke Huang et al. 2022. Few-Shot Model Agnostic Federated Learning. In *Proc. MM*. ACM, Lisboa, Portugal, 7309–7316.
- [15] Wenke Huang et al. 2022. Learn from Others and Be Yourself in Heterogeneous Federated Learning. In *Proc. CVPR*. IEEE, virtual, 10133–10143.
- [16] Sohei Itahara et al. 2023. Distillation-Based Semi-Supervised Federated Learning for Communication-Efficient Collaborative Training With Non-IID Private Data. *IEEE Trans. Mob. Comput.* 22, 1 (2023), 191–205.
- [17] Jaehye Jang et al. 2022. FedClassAvg: Local Representation Learning for Personalized Federated Learning on Heterogeneous Neural Networks. In *Proc. ICPP*. ACM, virtual, 76:1–76:10.
- [18] Eunjeong Jeong et al. 2018. Communication-Efficient On-Device Machine Learning: Federated Distillation and Augmentation under Non-IID Private Data. In *Proc. NeurIPS Workshop on Machine Learning on the Phone and other Consumer Devices*, virtual.
- [19] Peter Kairouz et al. 2021. Advances and Open Problems in Federated Learning. *Foundations and Trends in Machine Learning* 14, 1–2 (2021), 1–210.
- [20] Alex Krizhevsky et al. 2009. *Learning multiple layers of features from tiny images*. Toronto, ON, Canada, .
- [21] Daliang Li and Junpu Wang. 2019. FedMD: Heterogeneous Federated Learning via Model Distillation. In *Proc. NeurIPS Workshop*, virtual.
- [22] Qinbin Li et al. 2021. Practical One-Shot Federated Learning for Cross-Silo Setting. In *Proc. IJCAI*. ijcai.org, virtual, 1484–1490.
- [23] Paul Pu Liang et al. 2020. Think locally, act globally: Federated learning with local and global representations. *arXiv preprint arXiv:2001.01523* 1, 1 (2020).
- [24] Tao Lin et al. 2020. Ensemble Distillation for Robust Model Fusion in Federated Learning. In *Proc. NeurIPS*, virtual.
- [25] Chang Liu et al. 2022. Completely Heterogeneous Federated Learning. *CoRR* abs/2210.15865 (2022).
- [26] Xiaofeng Lu et al. 2022. Heterogeneous Model Fusion Federated Learning Mechanism Based on Model Mapping. *IEEE Internet Things J.* 9, 8 (2022), 6058–6068.
- [27] Ping Luo et al. 2019. Differentiable Learning-to-Normalize via Switchable Normalization. In *Proc. ICLR*. OpenReview.net, New Orleans, LA, USA, 1.
- [28] Disha Makhija et al. 2022. Architecture Agnostic Federated Learning for Neural Networks. In *Proc. ICML*, Vol. 162. PMLR, virtual, 14860–14870.
- [29] Brendan McMahan et al. 2017. Communication-Efficient Learning of Deep Networks from Decentralized Data. In *Proc. AISTATS*, Vol. 54. PMLR, Fort Lauderdale, FL, USA, 1273–1282.
- [30] Duy Phuong Nguyen et al. 2023. Enhancing Heterogeneous Federated Learning with Knowledge Extraction and Multi-Model Fusion. In *Proc. SC Workshop*. ACM, Denver, CO, USA, 36–43.
- [31] Jaehoon Oh et al. 2022. FedBABU: Toward Enhanced Representation for Federated Image Classification. In *Proc. ICLR*. OpenReview.net, virtual.
- [32] Sejun Park et al. 2023. Towards Understanding Ensemble Distillation in Federated Learning. In *Proc. ICML*, Vol. 202. PMLR, Honolulu, Hawaii, USA, 27132–27187.
- [33] Krishna Pillutla et al. 2022. Federated Learning with Partial Model Personalization. In *Proc. ICML*, Vol. 162. PMLR, virtual, 17716–17758.
- [34] Zhen Qin et al. 2023. FedAPEN: Personalized Cross-silo Federated Learning with Adaptability to Statistical Heterogeneity. In *Proc. KDD*. ACM, Long Beach, CA, USA, 1954–1964.
- [35] Felix Sattler et al. 2021. FEDAUx: Leveraging Unlabeled Auxiliary Data in Federated Learning. *IEEE Trans. Neural Networks Learn. Syst.* 1, 1 (2021), 1–13.
- [36] Felix Sattler et al. 2022. CFD: Communication-Efficient Federated Distillation via Soft-Label Quantization and Delta Coding. *IEEE Trans. Netw. Sci. Eng.* 9, 4 (2022), 2025–2038.
- [37] Aviv Shamsian et al. 2021. Personalized Federated Learning using Hypernetworks. In *Proc. ICML*, Vol. 139. PMLR, virtual, 9489–9502.
- [38] Tao Shen et al. 2020. Federated Mutual Learning. *CoRR* abs/2006.16765 (2020).
- [39] Yue Tan et al. 2022. FedProto: Federated Prototype Learning across Heterogeneous Clients. In *Proc. AAAI*. AAAI Press, virtual, 8432–8440.
- [40] Laurens van der Maaten and Geoffrey Hinton. 2008. Visualizing Data using t-SNE. *Journal of Machine Learning Research* 9, 86 (2008), 2579–2605.
- [41] Jiaqi Wang et al. 2023. Towards Personalized Federated Learning via Heterogeneous Model Reassembly. In *Proc. NeurIPS*. OpenReview.net, New Orleans, Louisiana, USA, 13.
- [42] Chuhan Wu et al. 2022. Communication-efficient federated learning via knowledge distillation. *Nature Communications* 13, 1 (2022), 2032.
- [43] Liping Yi, Gang Wang, Xiaoguang Liu, Zhuan Shi, and Han Yu. 2023. FedGH: Heterogeneous Federated Learning with Generalized Global Header. In *Proceedings of the 31st ACM International Conference on Multimedia (ACM MM'23)*. ACM, Canada, 11.
- [44] Fuxun Yu et al. 2021. Fed2: Feature-Aligned Federated Learning. In *Proc. KDD*. ACM, virtual, 2066–2074.
- [45] Sixing Yu et al. 2022. Resource-aware Federated Learning using Knowledge Extraction and Multi-model Fusion. *CoRR* abs/2208.07978 (2022).
- [46] Jie Zhang et al. 2021. Parameterized Knowledge Transfer for Personalized Federated Learning. In *Proc. NeurIPS*. OpenReview.net, virtual, 10092–10104.
- [47] Jianqing Zhang et al. 2023. FedCP: Separating Feature Information for Personalized Federated Learning via Conditional Policy. In *Proc. KDD*. ACM, Long Beach, CA, USA, 1.
- [48] Lan Zhang et al. 2022. FedZKT: Zero-Shot Knowledge Transfer towards Resource-Constrained Federated Learning with Heterogeneous On-Device Models. In *Proc. ICDCS*. IEEE, virtual, 928–938.
- [49] Zhilu Zhang and Mert R. Sabuncu. 2018. Generalized Cross Entropy Loss for Training Deep Neural Networks with Noisy Labels. In *Proc. NeurIPS*. Curran Associates Inc., Montréal, Canada, 8792–8802.
- [50] Zhuangdi Zhu et al. 2021. Data-Free Knowledge Distillation for Heterogeneous Federated Learning. In *Proc. ICML*, Vol. 139. PMLR, virtual, 12878–12889.
- [51] Zhuangdi Zhu et al. 2022. Resilient and Communication Efficient Learning for Heterogeneous Federated Systems. In *Proc. ICML*, Vol. 162. PMLR, virtual, 27504–27526.

A PSEUDO CODES OF FEDMOE

Algorithm 1: FedMoE

Input: N , total number of clients; K , number of sampled clients in one round; T , number of rounds; η_θ , learning rate of homogeneous feature extractor; η_ω , learning rate of local heterogeneous models; η_φ , learning rate of local homogeneous gating network.

Randomly initialize the global homogeneous feature extractor $\mathcal{G}(\theta^0)$, local personalized heterogeneous models $[\mathcal{F}_0(\omega_0^0), \mathcal{F}_1(\omega_1^0), \dots, \mathcal{F}_k(\omega_k^0), \dots, \mathcal{F}_{N-1}(\omega_{N-1}^0)]$ and local homogeneous gating networks $\mathcal{H}(\varphi^0)$.

for $t = 1$ **to** $T - 1$ **do**

// **Server Side:**

$\mathcal{S}^t \leftarrow$ Randomly sample $K \leq N$ clients to join FL;

Broadcast the global homogeneous feature extractor θ^{t-1} to sampled K clients;

$\theta_k^t \leftarrow$ **Client Update**(θ^{t-1});

/ Aggregate Homogeneous Feature Extractors */*

$$\theta^t = \sum_{k \in \mathcal{S}^t} \frac{n_k}{n} \theta_k^t.$$

// **Client Update:**

Receive the global homogeneous feature extractor θ^{t-1} from the server;

for $k \in \mathcal{S}^t$ **do**

for $(x_i, y_i) \in D_k$ **do**

$\theta_k^t \leftarrow$ **Client Update**(θ^{t-1});

/ Local MoE Training */*

$$\mathcal{R}_{k,i}^{\mathcal{G},t} = \mathcal{G}(x_i; \theta^{t-1}); \mathcal{R}_{k,i}^{\mathcal{F},t} = \mathcal{F}_k^{ex}(x_i; \omega_k^{ex,t-1});$$

$$[\alpha_{k,i}^{\mathcal{G},t}, \alpha_{k,i}^{\mathcal{F},t}] = \mathcal{H}(x_i; \varphi_k^{t-1});$$

$$\mathcal{R}_{k,i}^t = \alpha_{k,i}^{\mathcal{G},t} \cdot \mathcal{R}_{k,i}^{\mathcal{G},t} + \alpha_{k,i}^{\mathcal{F},t} \cdot \mathcal{R}_{k,i}^{\mathcal{F},t};$$

$$\hat{y}_i = \mathcal{F}_k^{hd}(\mathcal{R}_{k,i}^t; \omega_k^{hd,t-1});$$

$$\ell_i = CE(\hat{y}_i, y_i);$$

$$\theta_k^t \leftarrow \theta^{t-1} - \eta_\theta \nabla \ell_i;$$

$$\omega_k^t \leftarrow \omega_k^{t-1} - \eta_\omega \nabla \ell_i;$$

$$\varphi_k^t \leftarrow \varphi_k^{t-1} - \eta_\varphi \nabla \ell_i;$$

end

Upload trained local homogeneous feature extractor θ_k^t to the server.

end

end

Return personalized heterogeneous local complete models

$$[MoE(\mathcal{G}(\theta^{T-1}), \mathcal{F}_0^{ex}(\omega_0^{ex,T-1}); \mathcal{H}(\varphi_0^{T-1})) \& \mathcal{F}_0^{hd}(\omega_0^{hd,T-1}), \dots].$$

B THEORETICAL PROOFS

B.1 Proof for Lemma 1

An arbitrary client k 's local model W can be updated by $W_{t+1} = W_t - \eta g_{W,t}$ in the $(t+1)$ -th round, and following Assumption 1, we can obtain

$$\begin{aligned} \mathcal{L}_{tE+1} &\leq \mathcal{L}_{tE+0} + \langle \nabla \mathcal{L}_{tE+0}, (W_{tE+1} - W_{tE+0}) \rangle + \frac{L_1}{2} \|W_{tE+1} - W_{tE+0}\|_2^2 \\ &= \mathcal{L}_{tE+0} - \eta \langle \nabla \mathcal{L}_{tE+0}, g_{W,tE+0} \rangle + \frac{L_1 \eta^2}{2} \|g_{W,tE+0}\|_2^2. \end{aligned} \tag{20}$$

Taking the expectation of both sides of the inequality with respect to the random variable ξ_{tE+0} , we obtain

$$\begin{aligned}
\mathbb{E}[\mathcal{L}_{tE+1}] &\leq \mathcal{L}_{tE+0} - \eta \mathbb{E}[\langle \nabla \mathcal{L}_{tE+0}, g_{W,tE+0} \rangle] + \frac{L_1 \eta^2}{2} \mathbb{E}[\|g_{W,tE+0}\|_2^2] \\
&\stackrel{(a)}{=} \mathcal{L}_{tE+0} - \eta \|\nabla \mathcal{L}_{tE+0}\|_2^2 + \frac{L_1 \eta^2}{2} \mathbb{E}[\|g_{W,tE+0}\|_2^2] \\
&\stackrel{(b)}{\leq} \mathcal{L}_{tE+0} - \eta \|\nabla \mathcal{L}_{tE+0}\|_2^2 + \frac{L_1 \eta^2}{2} (\mathbb{E}[\|g_{W,tE+0}\|_2^2] + \text{Var}(g_{W,tE+0})) \\
&\stackrel{(c)}{=} \mathcal{L}_{tE+0} - \eta \|\nabla \mathcal{L}_{tE+0}\|_2^2 + \frac{L_1 \eta^2}{2} (\|\nabla \mathcal{L}_{tE+0}\|_2^2 + \text{Var}(g_{W,tE+0})) \\
&\stackrel{(d)}{\leq} \mathcal{L}_{tE+0} - \eta \|\nabla \mathcal{L}_{tE+0}\|_2^2 + \frac{L_1 \eta^2}{2} (\|\nabla \mathcal{L}_{tE+0}\|_2^2 + \sigma^2) \\
&= \mathcal{L}_{tE+0} + \left(\frac{L_1 \eta^2}{2} - \eta\right) \|\nabla \mathcal{L}_{tE+0}\|_2^2 + \frac{L_1 \eta^2 \sigma^2}{2}.
\end{aligned} \tag{21}$$

(a), (c), (d) follow Assumption 2. (b) follows $\text{Var}(x) = \mathbb{E}[x^2] - (\mathbb{E}[x])^2$.

Taking the expectation of both sides of the inequality with respect to the model W over E iterations, we obtain

$$\mathbb{E}[\mathcal{L}_{tE+1}] \leq \mathcal{L}_{tE+0} + \left(\frac{L_1 \eta^2}{2} - \eta\right) \sum_{e=1}^E \|\nabla \mathcal{L}_{tE+e}\|_2^2 + \frac{L_1 E \eta^2 \sigma^2}{2}. \tag{22}$$

B.2 Proof for Lemma 2

$$\begin{aligned}
\mathcal{L}_{(t+1)E+0} &= \mathcal{L}_{(t+1)E} + \mathcal{L}_{(t+1)E+0} - \mathcal{L}_{(t+1)E} \\
&\stackrel{(a)}{\approx} \mathcal{L}_{(t+1)E} + \eta \|\theta_{(t+1)E+0} - \theta_{(t+1)E}\|_2^2 \\
&\stackrel{(b)}{\leq} \mathcal{L}_{(t+1)E} + \eta \delta^2.
\end{aligned} \tag{23}$$

(a): we can use the gradient of parameter variations to approximate the loss variations, *i.e.*, $\Delta \mathcal{L} \approx \eta \cdot \|\Delta \theta\|_2^2$. (b) follows Assumption 3.

Taking the expectation of both sides of the inequality with respect to the random variable ξ , we obtain

$$\mathbb{E}[\mathcal{L}_{(t+1)E+0}] \leq \mathbb{E}[\mathcal{L}_{tE+1}] + \eta \delta^2. \tag{24}$$

B.3 Proof for Theorem 1

Substituting Lemma 1 into the right side of Lemma 2's inequality, we obtain

$$\mathbb{E}[\mathcal{L}_{(t+1)E+0}] \leq \mathcal{L}_{tE+0} + \left(\frac{L_1 \eta^2}{2} - \eta\right) \sum_{e=0}^E \|\nabla \mathcal{L}_{tE+e}\|_2^2 + \frac{L_1 E \eta^2 \sigma^2}{2} + \eta \delta^2. \tag{25}$$

B.4 Proof for Theorem 2

Interchanging the left and right sides of Eq. (25), we obtain

$$\sum_{e=0}^E \|\nabla \mathcal{L}_{tE+e}\|_2^2 \leq \frac{\mathcal{L}_{tE+0} - \mathbb{E}[\mathcal{L}_{(t+1)E+0}] + \frac{L_1 E \eta^2 \sigma^2}{2} + \eta \delta^2}{\eta - \frac{L_1 \eta^2}{2}}. \tag{26}$$

Taking the expectation of both sides of the inequality over rounds $t = [0, T-1]$ with respect to W , we obtain

$$\frac{1}{T} \sum_{t=0}^{T-1} \sum_{e=0}^{E-1} \|\nabla \mathcal{L}_{tE+e}\|_2^2 \leq \frac{\frac{1}{T} \sum_{t=0}^{T-1} [\mathcal{L}_{tE+0} - \mathbb{E}[\mathcal{L}_{(t+1)E+0}]] + \frac{L_1 E \eta^2 \sigma^2}{2} + \eta \delta^2}{\eta - \frac{L_1 \eta^2}{2}}. \tag{27}$$

Let $\Delta = \mathcal{L}_{t=0} - \mathcal{L}^* > 0$, then $\sum_{t=0}^{T-1} [\mathcal{L}_{tE+0} - \mathbb{E}[\mathcal{L}_{(t+1)E+0}]] \leq \Delta$, we can get

$$\frac{1}{T} \sum_{t=0}^{T-1} \sum_{e=0}^{E-1} \|\nabla \mathcal{L}_{tE+e}\|_2^2 \leq \frac{\frac{\Delta}{T} + \frac{L_1 E \eta^2 \sigma^2}{2} + \eta \delta^2}{\eta - \frac{L_1 \eta^2}{2}}. \tag{28}$$

If the above equation converges to a constant ϵ , *i.e.*,

$$\frac{\frac{\Delta}{T} + \frac{L_1 E \eta^2 \sigma^2}{2} + \eta \delta^2}{\eta - \frac{L_1 \eta^2}{2}} < \epsilon, \tag{29}$$

then

$$T > \frac{\Delta}{\epsilon(\eta - \frac{L_1\eta^2}{2}) - \frac{L_1E\eta^2\sigma^2}{2} - \eta\delta^2}. \tag{30}$$

Since $T > 0, \Delta > 0$, we can get

$$\epsilon(\eta - \frac{L_1\eta^2}{2}) - \frac{L_1E\eta^2\sigma^2}{2} - \eta\delta^2 > 0. \tag{31}$$

Solving the above inequality yields

$$\eta < \frac{2(\epsilon - \delta^2)}{L_1(\epsilon + E\sigma^2)}. \tag{32}$$

Since $\epsilon, L_1, \sigma^2, \delta^2$ are all constants greater than 0, η has solutions. Therefore, when the learning rate η satisfies the above condition, any client's local complete heterogeneous model can converge. Notice that the learning rate of the local complete heterogeneous model involves $\{\eta_\theta, \eta_\omega, \eta_\phi\}$, so it's crucial to set reasonable them to ensure model convergence. Since all terms on the right side of Eq. (28) except for Δ/T are constants, Δ is also a constant, FedMoE's non-convex convergence rate is $\epsilon \sim \mathcal{O}(\frac{1}{T})$.

C MORE EXPERIMENTAL DETAILS AND RESULTS

Table 4: Structures of 5 heterogeneous CNN models with 5×5 kernel size and 16 or 32 filters in convolutional layers.

Layer Name	CNN-1	CNN-2	CNN-3	CNN-4	CNN-5
Conv1	$5 \times 5, 16$	$5 \times 5, 16$	$5 \times 5, 16$	$5 \times 5, 16$	$5 \times 5, 16$
Maxpool1	2×2	2×2	2×2	2×2	2×2
Conv2	$5 \times 5, 32$	$5 \times 5, 16$	$5 \times 5, 32$	$5 \times 5, 32$	$5 \times 5, 32$
Maxpool2	2×2	2×2	2×2	2×2	2×2
FC1	2000	2000	1000	800	500
FC2	500	500	500	500	500
FC3	10/100	10/100	10/100	10/100	10/100
model size	10.00 MB	6.92 MB	5.04 MB	3.81 MB	2.55 MB

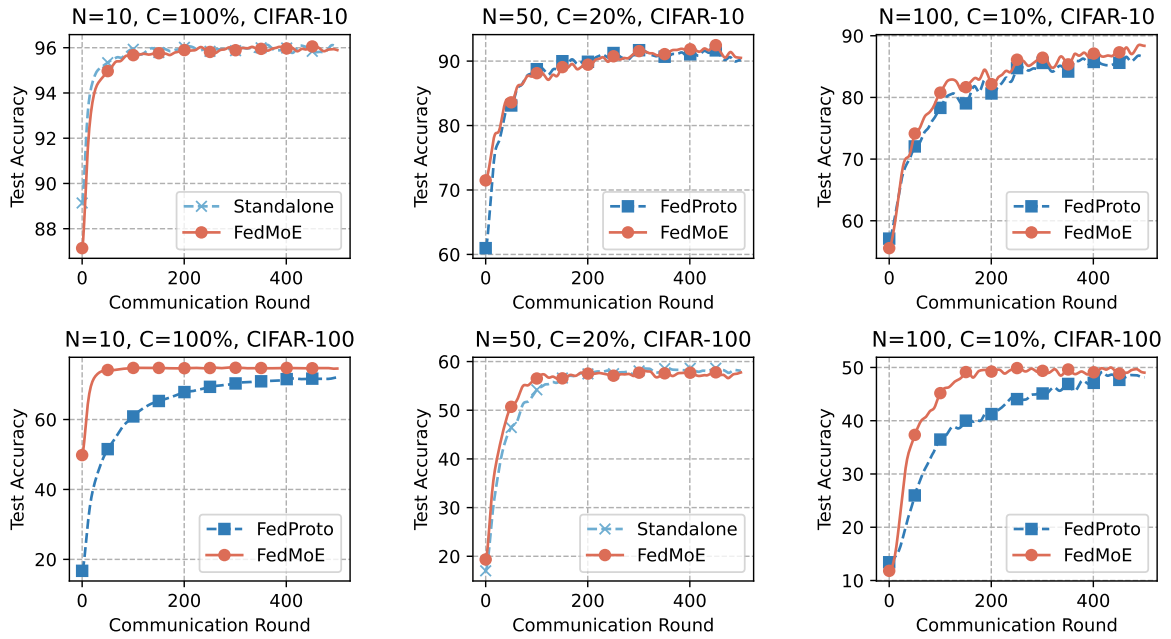


Figure 11: Average accuracy vs. communication rounds.